Age-Dependent Changes in Matrix Composition and Organization at the Ligament-to-Bone Insertion

I-Ning E. Wang,[1] Siddarth Mitroo,[1] Faye H. Chen,[4] Helen H. Lu,[1,2] and Stephen B. Doty[3]

[1]Biomaterials and Interface Tissue Engineering Laboratory, Department of Biomedical Engineering, Columbia University, 1210 Amsterdam Ave., 351 Engineering Terrace Bldg., MC8904, New York, New York 10027

[2]College of Dental Medicine, Columbia University, New York, New York 10032

[3]Analytical Microscopy Laboratory, The Hospital for Special Surgery, New York, New York 10021

[4]Cartilage Biology and Orthopaedics Branch, National Institute of Arthritis and Musculoskeletal and Skin Diseases, Department of Health and Human Services, National Institutes of Health, Bethesda, Maryland 20892

Received 29 September 2005; accepted 7 December 2005

Published online 15 June 2006 in Wiley InterScience (www.interscience.wiley.com). DOI 10.1002/jor.20149

ABSTRACT: Injuries to the anterior cruciate ligament (ACL) often occur at the ligament-to-bone insertion site; thus, an in-depth understanding of the native insertion is critical in identifying the etiology of failure and devising optimal treatment protocols for ACL injuries. The objective of this study is to conduct a systematic characterization of the ACL-to-bone interface, focusing on structural and compositional changes as a function of age. Using a bovine model, three age groups were studied: Neonatal (1–7 days old), Immature (2–6 months old), and Mature (2–5 years old). The distribution of types I, II, X collagen, decorin, cartilage oligomeric matrix protein (COMP), glycosaminoglycan (GAG), alkaline phosphatase (ALP) activity, and minerals at the ACL-to-bone insertion were examined. Additionally, cell aspect ratio, size, and distribution across the insertion were quantified. The ACL-to-bone insertion is divided into four regions: ligament, nonmineralized interface, mineralized interface, and bone. Both region-dependent and age-dependent structural and compositional changes at the insertion site were observed in this study. The interface in the skeletally immature group resembled articular cartilage, while the adult interface was similar to fibrocartilaginous tissue. Age-dependent changes in extracellular matrix composition (type X collagen, sulfated glycosaminoglycan), cellularity, ALP activity, and mineral distribution were also found. Marked differences in collagen fiber orientation between the femoral and tibial insertions were observed, and these differences became more pronounced with age. © 2006 Orthopaedic Research Society. Published by Wiley Periodicals, Inc. J Orthop Res 24:1745–1755, 2006

Keywords: aging; insertion; fibrocartilage; mineralization

INTRODUCTION

The anterior cruciate ligament (ACL) is a band of regularly oriented, dense connective tissue that connects the femur to the tibia. The ACL inserts into bone through an interface region, and serves as a joint stabilizer by acting as the primary restraint to anterior tibial translation. ACL tears and ruptures are the most common knee ligament injuries, and affect over 100,000 people per year in the United States alone.[1] Many ligament injuries occur at the ligament-to-bone insertion, particularly at the femoral insertion site.[2,3] As the ACL exhibits poor healing potential with its limited vascularization, ACL ruptures do not heal, and surgical intervention is required.[4–6] There are currently two autologous reconstruction options: bone-patella tendon-bone (BPB), and hamstring tendon-based grafts. Use of hamstring tendon-based grafts has increased due to limitations commonly associated with BPB grafts, for example, donor site morbidity, muscle atrophy, tendonitis, and arthritis.[7,8] However, the wider clinical utilization of the hamstring tendon-based graft is hindered by its inability to fully integrate with bone and the associated increase in knee laxity due to inadequate graft fixation.[8] Consequently, the extent of graft integration with osseous tissue remains the critical factor governing the long-term clinical outcome of soft tissue grafts. To address the challenge of soft tissue to bone integration, an in-depth understanding of the structural, chemical, and material properties of the native ACL-to-bone insertion site is needed.

The native ACL-to-bone insertion has been reported to consist of four different tissue regions:

Correspondence to: Helen H. Lu (Telephone: 212-854-4071; Fax: 212-854-8725; E-mail: h12052@columbia.edu)

ligament, nonmineralized interface, mineralized interface, and bone.[9–18] Specifically, the ligament region is composed of fibroblasts embedded in a type I and type III collagen matrix. The nonmineralized interface region consists of ovoid chondrocytes, and type II collagen is detectable within the pericellular matrix, and the primary sulfated proteoglycan is aggrecan. The mineralized interface region contains hypertrophic chondrocytes that are surrounded by extensive pericellular matrix.[14] Type X collagen, normally associated with hypertrophic chondrocytes, is found only within the mineralized region.[13,41] The gross appearance of the interface region has been reported to be similar to that of fibrocartilaginous tissue.[9] The last region along the ligament insertion axis is the subchondral bone, in which osteoblasts, osteocytes, and osteoclasts are embedded in a type I collagen matrix.

Previous characterization studies have provided valuable insight into the organization and composition of the interface. As such, current understanding of the soft tissue-to-bone insertion is derived based on findings from a variety of animal models (e.g., rat, bovine, rabbit, and human), in which neither species-specific nor age-dependent differences have been determined. There is thus a need for a systematic characterization of the interface in terms of matrix composition, component distribution, and mineralization within a single model. Moreover, the majority of the reported studies provided qualitative evaluations of the interface, and quantitative analyses of the variations, if any, in cellularity and cell size at the insertion have not been reported. Although the immediate postnatal development of the insertion site has been examined in the literature,[11,12,14,17] the age-dependent changes in insertion structure and matrix composition are not well understood. Knowledge of age-related changes at the insertion is crucial, because ACL injuries are largely reported in patients ranging 15 to 35 years of age.[19] An in-depth evaluation of the region-dependent and age-related changes at the insertion will be critical in our effort to regenerate the soft tissue-to-bone interface. Moreover, the interface between bone and tendons exhibits similar regional transitions described above; thus, findings from this study will augment current understanding of soft tissue-to-bone insertions.

The objective of this study is to conduct a systematic characterization of the ligament-to-bone interface as a function of age using both qualitative and quantitative methods applied to a single animal model. Analyses were performed for three age groups using a bovine model: Neonatal (1–7 days old), Immature (2–6 months old), and Mature (2–5 years old). It was hypothesized that there will be age-dependent changes in extracellular matrix composition, cellularity, and mineral distribution. The cell aspect ratio, size, and distribution across the four regions of the insertion were quantified, and the distribution of types I, II, X collagen, extracellular matrix proteins, and minerals were evaluated.

MATERIALS AND METHODS

All chemicals were purchased from Sigma Chemical (St. Louis, MO) unless otherwise noted.

Isolation of ACL-to-Bone Insertion Samples

Bovine knee joints were obtained from a local abattoir and the joints were divided into three groups: Neonatal, 1 to 7 days of age; Immature, 4 to 6 months of age; and Mature, 2 to 5 years of age. The joints ($n = 3$ per group) were cleaned in an antimicrobial bath. To isolate the insertion, a straight midline longitudinal incision extending from the distal femur to the tibia was made in the bovine knee under aseptic conditions. After retraction of skin and subcutaneous fascia, the patellar tendon was removed, and a deeper incision was made into the joint capsule to expose the femoral condyle and the tibial plateau. The femoral and tibial insertions were identified and excised. The sample comprised of the ligament and intact insertion connected to the bony regions. The samples were rinsed with phosphate-buffered saline (PBS), fixed in 10% neutral buffered formalin plus 1% cetylpyridium chloride for 4 h, and stored in PBS at 4°C prior to processing.

Preparation of Nondecalcified and Decalcified Samples

For immunohistochemistry and histology, the samples were first decalcified in 5% formic acid. Samples were cut sagittally to expose the insertion site and then processed for paraffin embedding (Tissue Tek VIP Tissue Processor, Sakura Finetek U.S.A., Inc., Torrance, CA), sectioned to 5 μm in thickness, and prepared for standard histology or immunohistochemistry. To localize the mineral distribution at the insertion site, frozen sections were prepared. Briefly, mineralized insertion sites were cryoprotected with a 5% polyvinyl alcohol solution and frozen sections (8 μm) were obtained using a tungsten-carbide knife (Hacker Instrument, Inc., Fairfield, NJ). The sections were air dried or stabilized in absolute acetone prior to staining.

Extracellular Matrix Organization—Total Collagen and Proteoglycans

Matrix distribution was assessed using the Modified Goldner's Masson Trichrome Stain.[20] Total collagen

distribution was visualized by Picro Sirius stain, where the samples were immersed in 0.1% Sirius Red solution and counterstained with Harris' Hematoxylin. The insertion of collagen fibers at the interface was visualized using a polarized light filter.[21] Matrix proteoglycan distribution was detected by 1% Alcian Blue stain in 3% acetic acid followed by Kernechtrot counterstaining.

Extracellular Matrix Distribution—Collagen I, II, X, Decorin, COMP

The distribution of types I, II, X collagen, and matrix proteins such as decorin and cartilage oligomeric matrix protein (COMP) were evaluated using immunohistochemistry. Monoclonal antibodies for type II collagen (1:20 dilution), type X collagen (undiluted), and decorin (undiluted) were purchased from Developmental Studies Hybridoma Bank (Iowa City, IA). Murine monoclonal antibody against type I collagen was purchased from Chemicon International, Inc. (Temecula, CA) and used at 1:60 dilution. Polyclonal antibody F8 against COMP was used at 1:1000 dilution. Parallel negative controls were run with PBS substituting primary antibodies. Before staining for decorin and types II and X collagen, the samples were treated with 1% hyaluronidase for 30 min at 37°C, and then incubated with primary antibody overnight. Following PBS wash, biotinylated secondary antibody and Streptavidin conjugate (LSAB 2 System, DAKO, Carpinteria, CA, and Vectastain kit, Fisher Scientific, Fair Lawns, NJ) were added. Positive staining with the colorimetric substrate 3,3′ Diaminobenzidine or N,N′ Dimethylformamide was indicated by the formation of brown precipitates.

Alkaline Phosphatase (ALP) Activity and Mineral Distribution at the ACL-to-Bone Insertion

The staining to ALP activity[22] was performed on the cryosectioned samples immediately following sectioning. The samples were fixed in acetone and incubated in the ALP solution (Fast Blue RR Salt) for 30 min. The samples were counterstained with Eosin prior to viewing. The mineralized region at the interface was visualized by Von Kossa staining.[23] The samples were immersed in 5% silver nitrate solution and exposed to ultraviolet light for 10 min to initiate the reaction. The samples were then rinsed with water and viewed using light microscopy (Zeiss Axiovert 25, Zeiss, Germany).

Quantitative Analyses of Insertion—Interfacial Thickness, Cell Density, Area, Aspect Ratio

Light microscopy images of the insertion site were evaluated using customized digital image analyses (Scion Image, Frederick, MD). Interfacial thickness ($n = 3$), which pertains to the interface region of the insertion, was quantified using trichrome staining images. Image calibration was performed by correlating the spanning pixel value to the length of the scale bar. Each image was divided into nine regions perpendicular to the insertion orientation, and an average thickness was computed across the insertion. Cell density at the interface ($n = 3$) was measured based on the hematoxylin and eosin staining images. The interface was divided into nine subdivisions progressing in parallel from ligament to bone, and the number of cell nuclei was counted across each division and summed. Change in cell aspect ratio across the interface ($n = 3$) was computed by determining the ratio of the major and minor axes of each cell, while cell cross-sectional area ($n = 3$) was calculated assuming an elliptic geometry. Cell aspect ratio and area were calculated based on the Neonatal and Immature groups, as cellularity was difficult to visualize in the Mature group due to the dense distribution of fibrocartilage at the interface.

Statistical Analysis

Data are expressed as mean ± standard deviation. For statistical analysis, a two-way analysis of variance was performed to determine the interface thickness, cell density, area, and aspect ratio. The Tukey-Kramer post hoc test was used for all pairwise comparisons, and statistical significance was set at $p < 0.05$. All statistical analyses were performed using the JMP statistical software package (SAS Institute, Cavy, NC).

RESULTS

Extracellular Matrix Organization

Three distinct regions were observed, and will be referred to here as: Ligament, Interface, and Bone (Fig. 1A). The Interface is further divided into the NonMineralized Interface and Mineralized Interface regions. The width and organization of the interface varied as a function of age. Specifically, interfacial morphology in the Neonatal group (Fig. 1A1) and Immature group (Fig. 1A2) resembled those of articular cartilage, while the Interface region in the Mature group (Fig. 1A3) was found to be more fibrocartilage-like, with chondrocytes distributed along the long axis of the collagen fibers. Blood vessels were observed in the Interface region and the Bone region. Interfacial thickness was 780 ± 3 μm for the Neonatal group, followed by 480 ± 5 μm for the Immature group and 356 ± 4 μm for the Mature group. Significant difference in interfacial thickness was found among the three age groups examined ($p < 0.05$).

Individual cell cross-sectional area increased from the Ligament region to the Bone region. Ligament fibroblasts were elongated and aligned along the long axis of the collagen fibers, while cells at the Interface region exhibited a spherical-shaped, chondrocyte-like morphology. Hypertrophic chondrocytes were clustered at the

Mineralized Interface region. Additionally, cross-sectional cell area increased from the Ligament region to Bone (Fig. 1B). For the Neonatal group, cell area was the greatest near the Bone region at $510 \pm 79\ \mu m^2$, and it decreased away from Bone to the Ligament region ($127 \pm 32\ \mu m^2$). For Immature group, cell area near bone tissue measured $694 \pm 178\ \mu m^2$, and $262 \pm 88\ \mu m^2$ near the ligament. No significant difference in cell density and aspect ratio was observed with age. Cell density remained constant across the insertion, while region-dependent changes in cell cross-sectional area and aspect ratio were found. Cell aspect ratio was the highest within the Ligament region (1.6 ± 0.3) compared to the other regions ($p < 0.05$).

Collagen Distribution and Insertion into the Interface Region

In the Neonatal and Immature groups, a near 90° bend in collagen fiber orientation was observed near the Interface region, with the collagen bundles aligned parallel to the interface (Fig. 2A1). Under polarized light, an oblique insertion of several strands of collagen fibers from the Ligament to the Interface region was observed (Fig. 2A2). In contrast, for the Mature group, the collagen fibers inserted continuously and perpendicularly into the Interface region (Fig. 2C2). The alignment of the collagen bundles in the Ligament region remained parallel to that of the Interface region. Differences in fiber orientation were also

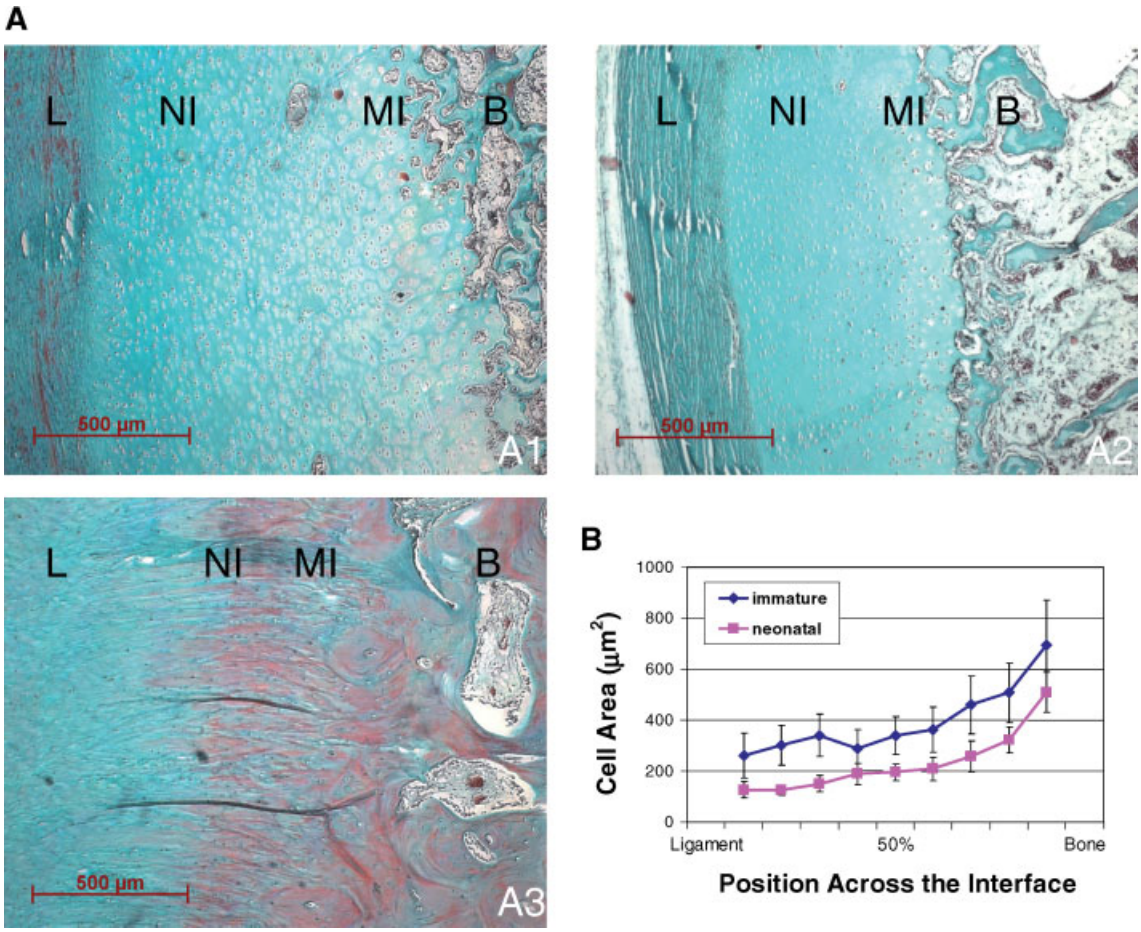

Figure 1. Age-dependent changes in the matrix and cellular organization at the ACL-to-bone insertion. The insertion can be divided into three regions: Ligament (L), Interface, and Bone (B). The Interface region is further divided into the Nonmineralized (NI) and Mineralized (MI) Interface regions. (A) Structural organization, Goldner's Trichrome: (1) Neonatal, 1 to 7 days of age; (2) Immature, 4 to 6 months of age; and (3) Mature, 2 to 5 years of age. Interface morphology in the Neonatal and Immature groups resembles those of articular cartilage, while the Mature Interface is more fibrous and fibrocartilage-like, suggesting significant adaptation occurred with maturation. (B) Region-dependent variation in cell area reflects the change in cellularity across the insertion, from fibroblasts to chondrocytes, and then to hypertrophic chondrocytes.

 DOI 10.1002/jor

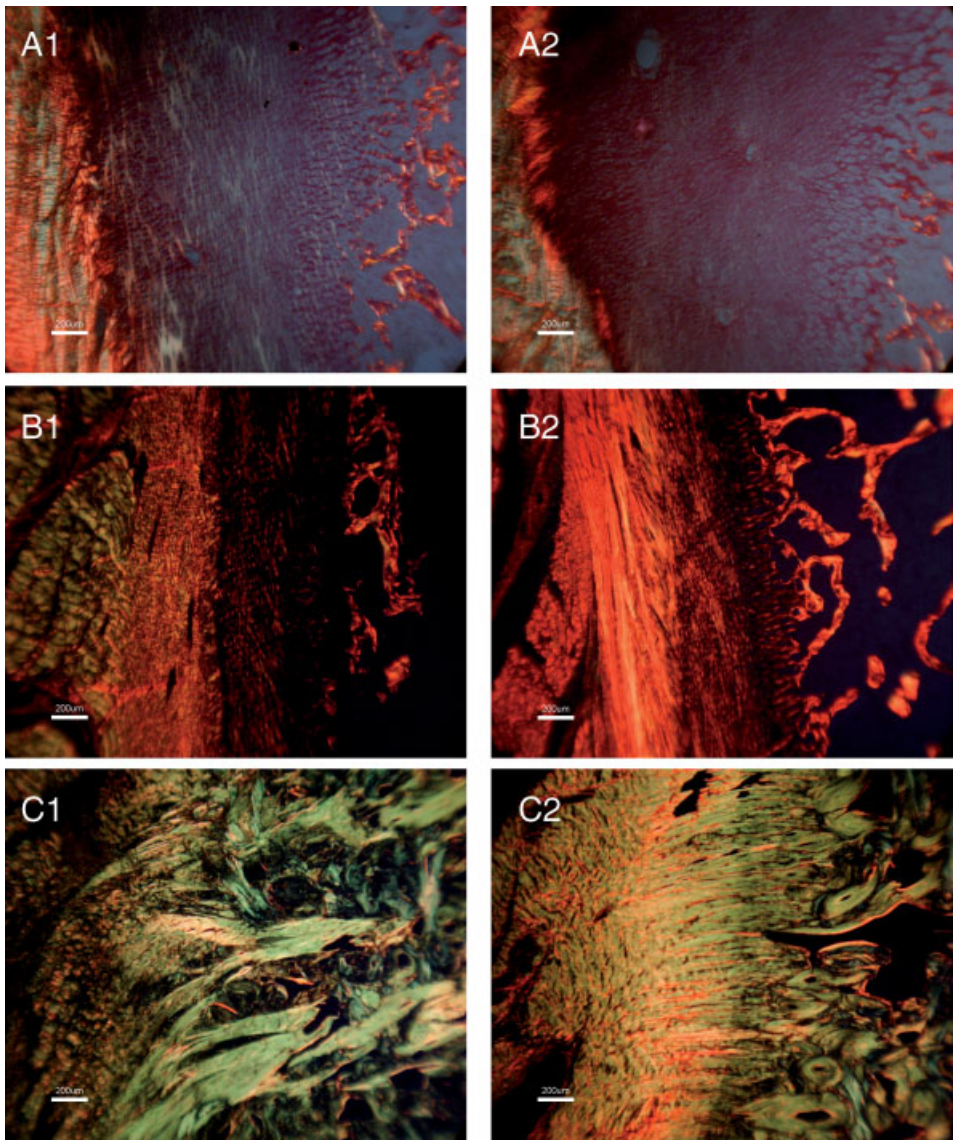

Figure 2. Insertion- and age-dependent changes in collagen insertion patterns. Picro Sirius Red staining combined with circular polarized light microscopy on Femoral (1-left) and Tibial (2-right) insertions. (A) Neonatal; (B) Immature; (C) Mature, bar = 200 μm. The collagen fibers at the tibial insertion are more organized compare to those of the femoral insertion site. These differences also become more pronounced with maturation.

observed between the femoral and tibial insertions. Fiber orientation at the tibial insertion was more uniform (Fig. 2C2) with the fibers aligned in parallel to each other, while the collagen fibers found at the femoral insertion (Fig. 2C1) were much less organized. The highest stain intensity for type I collagen was observed in the Ligament region. Type II collagen was located mainly in the Interface region, with higher intensity stain found at the Mineralized Interface region (Fig. 3A). No discernable differences were observed with age.

Extracellular Matrix Proteins and Proteoglycan Distribution

No observable differences in decorin or COMP distribution were found as a function of age. Decorin was located largely in the Ligament and Interface regions, and COMP was observed primarily pericellularly in the Interface region (Fig. 3B). In contrast, both age-dependent and region-dependent changes in proteoglycan distribution were observed across the insertion. Positive glycosaminoglycan (GAG) staining was found at the Interface region, and the intensity of the stain decreased

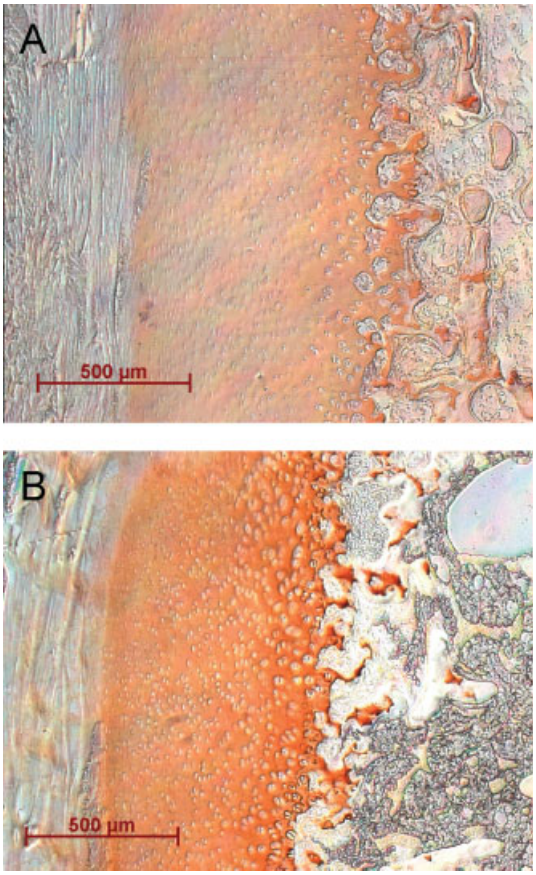

Figure 3. The distribution of type II collagen and cartilage oligomeric matrix protein (COMP) remained unchanged with age. Immunohistochemical staining for (A) Type II collagen, and (B) COMP in the Immature group. Type II collagen was observed in the Interface region for all age groups, and the Mineralized Interface region exhibited higher intensity of type II collagen stain. Similarly, COMP was found in the Interface region for all age groups examined.

consistently with increasing age (Fig. 4). Proteoglycan content in the Immature (Fig. 4A2) and Mature (Fig. 4A3) groups were markedly lower compared to the Neonatal (Fig. 4A1). For the Neonatal group, more intense GAG staining was associated with the mineralized interface region, within the matrix surrounding the hypertrophic chondrocytes.

Type X Collagen, ALP Activity, and Mineral Distribution

Type X collagen distribution at the insertion was both region- and age-dependent. It was localized exclusively in the Mineralized Interface region (Fig. 5A), and associated in a relatively thin layer with hypertrophic chondrocytes in both the Neonatal (Fig. 5A1) and Immature (Fig. 5A2) groups.

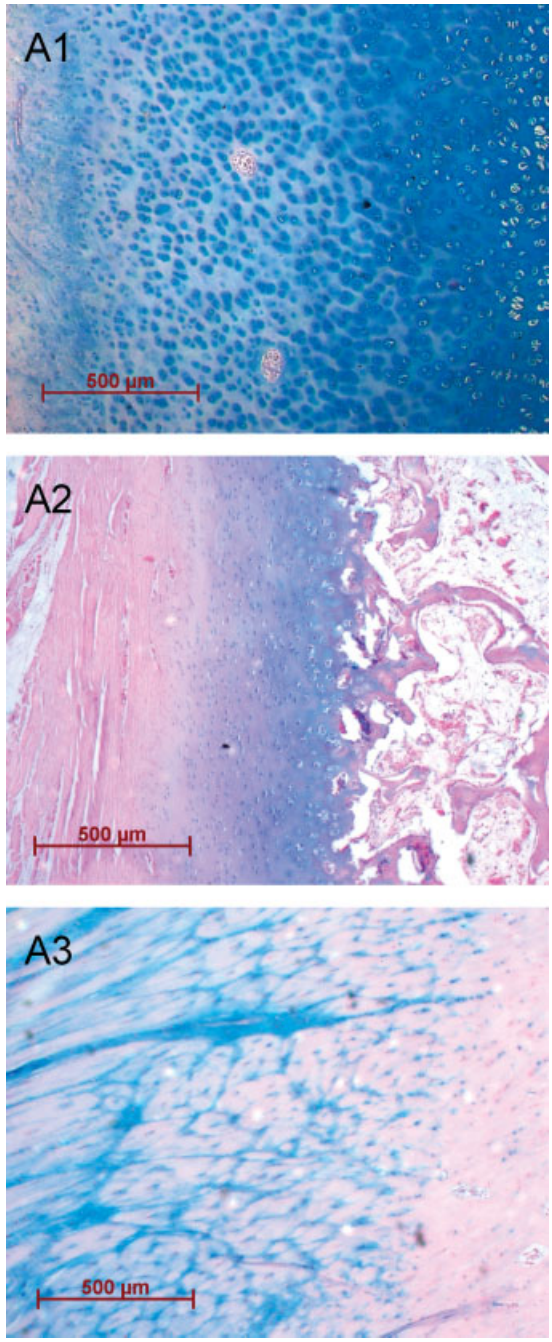

Figure 4. Proteoglycan distribution at the insertion as a function of age. Alcian Blue staining: (A1) Neonatal, (2) Immature, and (3) Mature. Proteoglycans are found in the Interface region for all age groups, and the staining intensity decreases with age, which is consistent with the formation of a fibrocartilage-like interface in the Mature group.

Type X collagen distribution increased with skeletal maturity, and positive staining was observed across the Interface region for the Mature group (Fig. 5A3).

 DOI 10.1002/jor

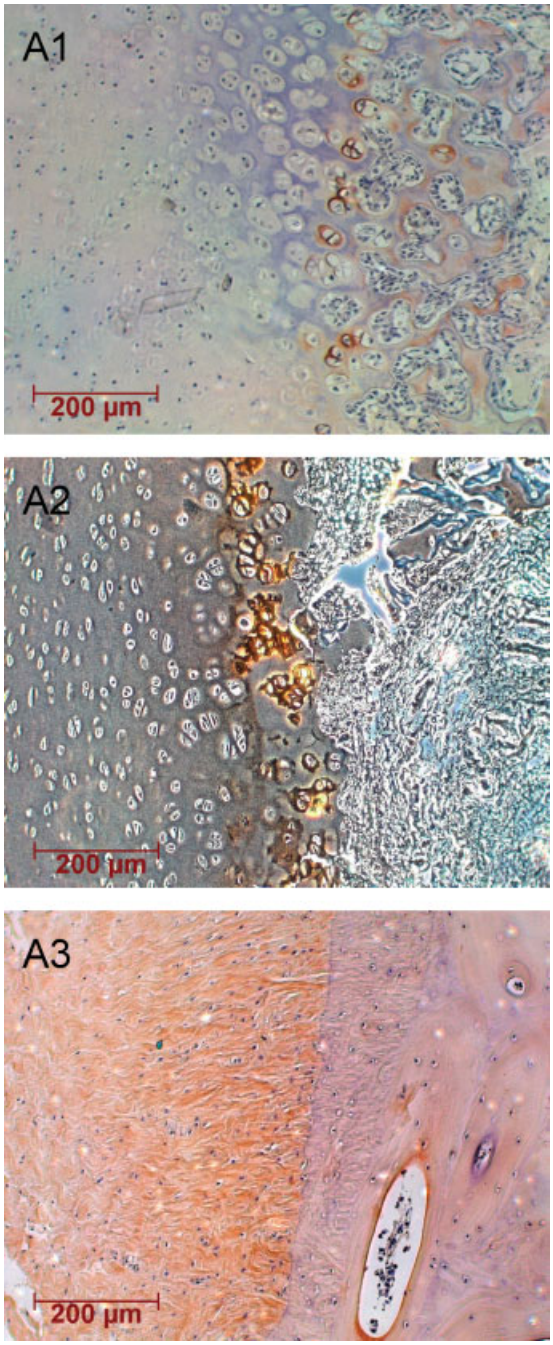

Figure 5. Age-dependent changes in type X collagen deposition at the ACL-to-bone insertion. Immunohistochemical staining for type X collagen: (A1) Neonatal, (2) Immature, and (3) Mature. Type X collagen is found exclusively in the Mineralized Interface region in the Neonatal and Immature groups, especially within the matrix surrounding hypertrophic chondrocytes. The Neonatal group exhibits the lowest type X collagen staining, while the highest staining intensity is found in the Interface region of the Mature group.

The strongest ALP activity (in blue) was found at the Bone region, and positive staining was also observed in the Interface (Fig. 6A). The ALP activity in both the Bone and Interface regions decreased with age, with the highest enzyme activity seen at the Interface region of the Neonatal group (Fig. 6A1), followed by the Immature and Mature groups. ALP activity became localized in the Mineralized Interface region with age, while greater staining intensity was associated with the hypertrophic chondrocytes in the Neonatal group. Mineral distribution at the insertion was both region- and age-dependent. For the Neonatal group (Fig. 6B1), Von Kossa staining (in black) showed highly positive and dense phosphate intensity at the Bone region and surrounding the hypertrophic chondrocytes. No mineral was detected in the Ligament or Nonmineralized Interface regions. As the animal aged, mineral distribution became increasingly localized in the Mineralized Interface and Bone regions (Fig. 6B2 and 6B3). In addition, the mineral density for the Mature group was greater compared to the two other age groups examined in this study.

DISCUSSION

We have conducted a systematic characterization of the matrix organization, composition and mineral distribution at the ligament-to-bone insertion, and have found both region- and age-dependent changes across the insertion site. The ACL inserts into bone through a gradual transition from the Ligament region to a Nonmineralized Interface region, followed by a Mineralized Interface region and then the Bone region. Matrix proteins commonly associated with the insertion include collagen types I, II, III, and X, GAG and decorin.[24–26] Type I collagen was observed in all four regions in this study, and its distribution did not vary significantly with age. Niyibizi et al. examined type I collagen distribution in mature bovine medial collateral ligament insertion, and found that type I collagen was located primarily in the Ligament and Bone regions.[27] Type I collagen was also found in the Interface region of adult rat supraspinatus tendon.[8]

COMP is a member of the thrombospondin family of proteins.[28] It was first identified in cartilage,[29] and has been reported in tendons at regions of compression and tension.[30] In this study, COMP was observed in both the Mineralized and Nonmineralized Interface regions, and continued to be present as the animal matured. Occasionally,

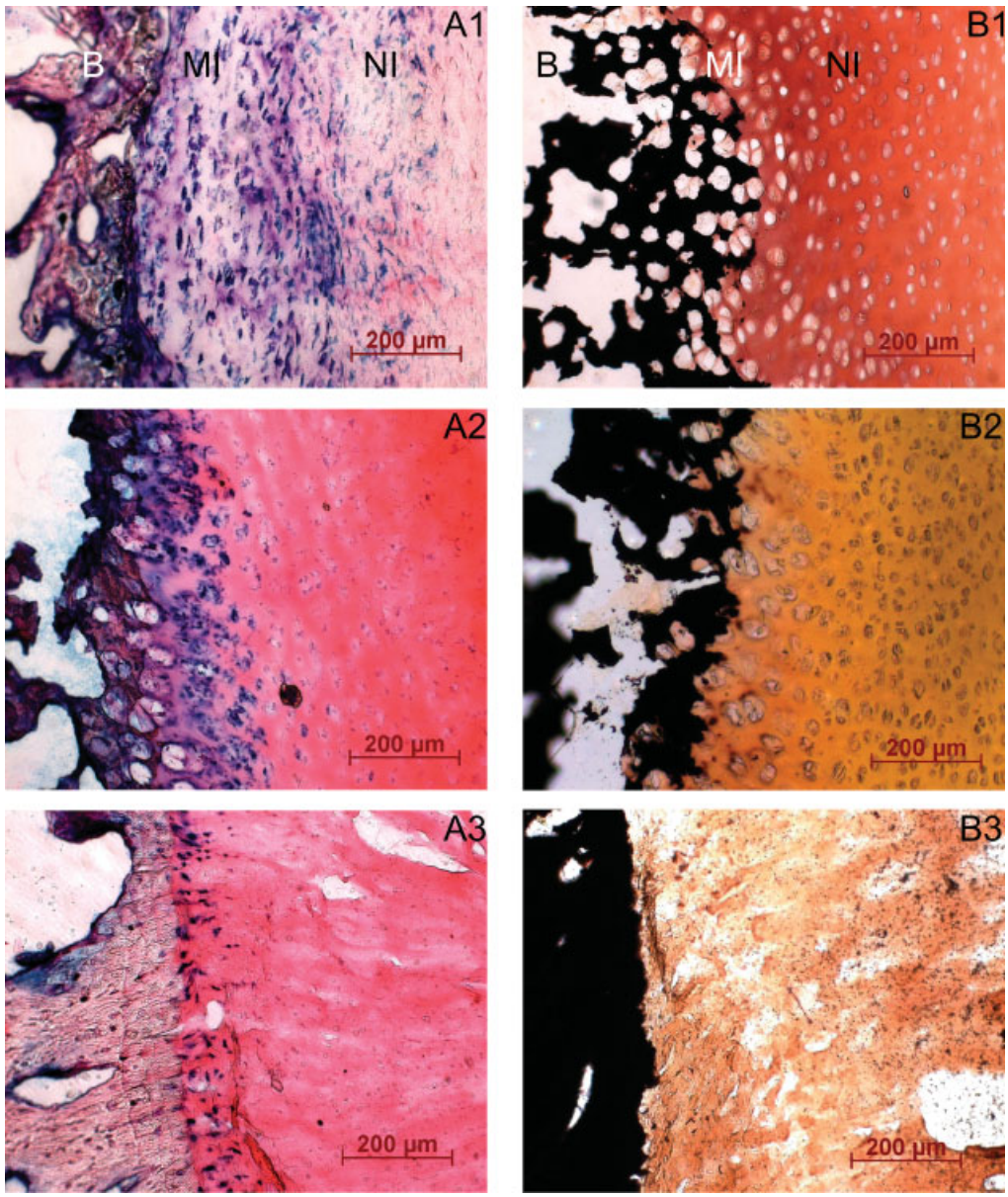

Figure 6. Age-dependent changes in alkaline phosphatase (ALP) activity and mineral distribution at the ACL-to-bone insertion. (A) ALP activity, and (B) Mineral distribution via Von Kossa staining, with (1) Neonatal, (2) Immature, and (3) Mature. The ALP activity is the highest in the Neonatal group, followed by the Immature and the Mature group. For the Mature group, ALP activity is present only in the Mineralized Interface region. Mineralization is located in the Mineralized Interface and Bone regions for all age groups, and mineral staining intensity increased with age.

higher intensity stain was seen at the juncture between the Ligament and the Interface regions as well as between the Interface and the Bone regions. This is likely related to significant changes in the nature of mechanical stress progressing from ligament to fibrocartilage and from mineralized fibrocartilage to bone. The COMP protein may play a role in mechanotransduction across the interface, and its effect will be investigated in future studies.

Age-dependent changes in both the thickness and structural organization of the insertion were found in this study. Interestingly, a hyaline cartilage-like interface was observed in the Neonatal and Immature groups, while a fibrocartilage-like interface[31] was found in the skeletally Mature group. Hypertrophic chondrocytes were distributed in clusters with a pericellular matrix containing types II and X collagen in all age groups

 DOI 10.1002/jor

examined. In general, cell aspect ratio decreased from the Ligament region to Bone, representing the change from elongated fibroblasts to spherical chondrocytes, followed by hypertrophic chondrocytes of the Mineralized Interface region. These age-dependent changes suggest an active remodeling of the interface over time, with the primary modulator being the nature and magnitude of physiological loading experienced at the insertion during maturation.

Both regional and age-dependent changes in proteoglycan or GAG distribution were found at the insertion. Sulfated GAG was primarily observed at the Interface regions, with intense GAG stain observed in the Neonatal group. Proteoglycan presence at the interface diminished as the interface matured. The mode of collagen insertion across the interface varied as a function of age. The oblique insertion of collagen fibers found immediately postnatal were absent in the skeletally mature animal, replaced by a more organized insertion with continuous collagen fibers traversing the Interface region and perpendicular to the Bone region. This specific orientation of the collagen fibers is likely reflective of the direction of tensile loading found across the insertion site.

It is well established that the Interface region consists of a linear transition from nonmineralized to mineralized tissue.[11,13,32–36] The demarcation between these two interfacial regions is often difficult to define; thus, several methods were used in this study to delineate these two regions. ALP activity, type X collagen distribution, and phosphate distribution were examined across the interface region. ALP is an enzyme required in cell-mediated mineralization, and type X collagen, synthesized by hypertrophic chondrocytes, is an important marker for endochondral ossification. We found a thin layer of type X collagen surrounding hypertrophic chondrocytes, and areas of ALP activity and mineral distribution corresponded to the mineralized regions.

It has long been postulated that the principal function of the insertion site between bone and soft tissue is to minimize the formation of stress concentrations, and to facilitate stress transfer between these two distinct types of tissue.[2,37] The observed sequential arrangement across the insertion from ligament to nonmineralized interface, followed by the mineralized interface and finally bone will likely result in an increase in mineral content. Preliminary results from our group demonstrated that the mechanical properties at the ligament bone interface were region-dependent, with an increase in elastic modulus from the nonmineralized to the mineralized interface region in the Neonatal group.[38] We believe that the progression from soft-to-hard tissue facilitated a gradual change in stiffness across the interfacial regions, effectively lowering the stress concentration at the insertion sites. Higher ALP activity was found in the Neonatal and Immature groups, suggesting the potential for mineralization and the ability of the growing interface to adapt to physiological loading. The increase in mineral density with age is indicative of the maturation of the calcium phosphate matrix, providing further evidence that the interface undergoes adaptation.

Considering Wolff's law[39] and the structure–function relationship of biological tissues, we believe the findings of this study collectively suggest that the composite organization of the Mature insertion, in which highly oriented collagen fiber are embedded in a proteoglycan matrix, is the result of adaptation to the stress distribution or physiological loading present at the interface. Applied tensile loading may expose insertions to tensile, shear, and compressive stresses, and ultrasound elastography analysis revealed that both compressive and tensile strains are present at this insertion site.[16,40] The tensile stress at the interface is likely transmitted by the collagen fibers, while the proteoglycan and type II collagen-rich matrix will transmit the compressive loads. These results suggest a dynamic stress profile, which varies as a function of age. It is possible that during maturation, the accumulated mechanical loading at the insertion is age dependent, resulting in adaptation in matrix organization and composition at the interface.

In summary, through a systematic characterization of the interface, both region-dependent as well as age-dependent changes in matrix organization and composition were found at the ligament-to-bone insertion site. Future studies will focus on elucidating the structure–function relationship existing at this and other soft tissue-to-bone interfaces.

ACKNOWLEDGMENTS

The authors gratefully acknowledge Ms. Orla O'Shea from the Analytical Microscopy Laboratory of the Hospital for Special Surgery for assistance with histology preparation and Mr. Vincent Rubino of Columbia University for assistance with image analyses. The monoclonal antibodies II-II6B3 and X-AC9 developed by TF Linsenmayer and monoclonal antibody DS1 developed by AR Poole were obtained from the Developmental Studies Hybridoma Bank developed under the auspices

of the NICHD and maintained by the University of Iowa, Department of Biological Science, Iowa City, IA 52242. This study was funded by an award from NIH-NIAMS (1R21 AR052402-01A1HHL).

REFERENCES

1. Jackson DW, Heinrich JT, Simon TM. 1994. Biologic and synthetic implants to replace the anterior cruciate ligament. Arthroscopy 10:442–452.
2. Gao J, Rasanen T, Persliden J, et al. 1996. The morphology of ligament insertions after failure at low strain velocity: an evaluation of ligament entheses in the rabbit knee. J Anat 189:127–133.
3. Noyes FR, DeLucas JL, Torvik PJ. 1974. Biomechanics of anterior cruciate ligament failure: an analysis of strain-rate sensitivity and mechanisms of failure in primates. J Bone Joint Surg Am 56:236–253.
4. Daniel DM, Stone ML, Dobson BE, et al. 1994. Fate of the ACL-injured patient. A prospective outcome study. Am J Sports Med 22:632–644.
5. Noyes FR, Mangine RE, Barber S. 1987. Early knee motion after open and arthroscopic anterior cruciate ligament reconstruction. Am J Sports Med 15:149–160.
6. Tom JA, Rodeo SA. 2002. Soft tissue allografts for knee reconstruction in sports medicine. Clin Orthop 402:135–156.
7. Barrett GR, Noojin FK, Hartzog CW, et al. 2002. Reconstruction of the anterior cruciate ligament in females: a comparison of hamstring versus patellar tendon autograft. Arthroscopy 18:46–54.
8. Beynnon BD, Johnson RJ, Fleming BC, et al. 2002. Anterior cruciate ligament replacement: comparison of bone–patellar tendon–bone grafts with two-strand hamstring grafts. A prospective, randomized study. J Bone Joint Surg Am 84-A:1503–1513.
9. Benjamin M, Ralphs JR. 2001. Entheses—the bony attachments of tendons and ligaments. Ital J Anat Embryol 106(2 Suppl 1):151–157.
10. Clark JM, Sidles JA. 1990. The interrelation of fiber bundles in the anterior cruciate ligament. J Orthop Res 8:180–188.
11. Messner K. 1997. Postnatal development of the cruciate ligament insertions in the rat knee. Morphological evaluation and immunohistochemical study of collagens types I and II. Acta Anat 160:261–268.
12. Nawata K, Minamizaki T, Yamashita Y, et al. 2002. Development of the attachment zones in the rat anterior cruciate ligament: changes in the distributions of proliferating cells and fibrillar collagens during postnatal growth. J Orthop Res 20:1339–1344.
13. Niyibizi C, Sagarrigo VC, Gibson G, et al. 1996. Identification and immunolocalization of type X collagen at the ligament–bone interface. Biochem Biophys Res Commun 222:584–589.
14. Petersen W, Tillmann B. 1999. Structure and vascularization of the cruciate ligaments of the human knee joint. Anat Embryol (Berl) 200:325–334.
15. Sagarriga VC, Kavalkovich K, Wu J, et al. 1996. Biochemical analysis of collagens at the ligament–bone interface reveals presence of cartilage-specific collagens. Arch Biochem Biophys 328:135–142.
16. Thomopoulos S, Williams GR, Gimbel JA, et al. 2003. Variations of biomechanical, structural, and compositional properties along the tendon to bone insertion site. J Orthop Res 21:413–419.
17. Wei X, Messner K. 1996. The postnatal development of the insertions of the medial collateral ligament in the rat knee. Anat Embryol (Berl) 193:53–59.
18. Woo S, An K, Frank CB. 2000. Anatomy, biology, and biomechanics of tendon and ligament. In: Buckwalter JA, Einhorn TA, Simon SR, editors. Orthopaedic basic science. 2nd ed. Rosemont: American Academy of Orthopaedic Surgery. p 581–616.
19. Seil R, Kohn D. 2000. Ruptures of the anterior cruciate ligament (ACL1) during growth. Bull Soc Sci Med Grand Duche Luxemb 39–53.
20. Gruber H. 1992. Adaptations of Goldner's Masson trichrome stain for the study of undecalcified plastic embedded bone. Biotech Histochem 67:30–34.
21. Junqueira LC, Bignolas G, Brentani RR. 1979. Picrosirius staining plus polarization microscopy, a specific method for collagen detection in tissue sections. Histochem J 11:447–455.
22. Kaplow LS. 1955. A histochemical procedure for localizing and evaluating leukocyte alkaline phosphatase activity in smears of blood and marrow. Blood 10:1023–1029.
23. von Kossa J. 1901. Uber die im organismus kunstlich erzeugen verkalkungen. Beitr Path Anat 29:163–202.
24. Krusius T, Ruoslahti E. 1986. Primary structure of an extracellular matrix proteoglycan core protein deduced from cloned cDNA. Proc Natl Acad Sci USA 83:7683–7687.
25. Scott JE, Orford CR. 1981. Dermatan sulphate-rich proteoglycan associates with rat tail-tendon collagen at the d band in the gap region. Biochem J 197:213–216.
26. Vogel KG, Paulsson M, Heinegard D. 1984. Specific inhibition of type I and type II collagen fibrillogenesis by the small proteoglycan of tendon. Biochem J 223:587–597.
27. Niyibizi C, Visconti CS, Kavalkovich K, et al. 1995. Collagens in an adult bovine medial collateral ligament: immunofluorescence localization by confocal microscopy reveals that type XIV collagen predominates at the ligament–bone junction. Matrix Biol 14:743–751.
28. Oldberg A, Antonsson P, Lindblom K, et al. 1992. COMP (cartilage oligomeric matrix protein) is structurally related to the thrombospondins. J Biol Chem 267:22346–22350.
29. Hedbom E, Antonsson P, Hjerpe A, et al. 1992. Cartilage matrix proteins. An acidic oligomeric protein (COMP) detected only in cartilage. J Biol Chem 267:6132–6136.
30. Smith RK, Zunino L, Webbon PM, et al. 1997. The distribution of cartilage oligomeric matrix protein (COMP) in tendon and its variation with tendon site, age and load. Matrix Biol 16:255–271.
31. Mow VC, Ratcliffe A. 1997. Structure and function of articular cartilage and meniscus. In: Mow VC, Hayes WC, editors. Basic orthopaedic biomechanics. 2nd ed. Philadelphia: Lippincott-Raven. p 113–177.
32. Benjamin M, Evans EJ, Rao RD, et al. 1991. Quantitative differences in the histology of the attachment zones of the meniscal horns in the knee joint of man. J Anat 177:127–134.
33. Benjamin M, Kumai T, Milz S, et al. 2002. The skeletal attachment of tendons—tendon "entheses." Comp Biochem Physiol A Mol Integr Physiol 133:931–945.
34. Bloebaum RD, Kopp DV. 2004. Remodeling capacity of calcified fibrocartilage of the hip. Anat Rec A Discov Mol Cell Evol Biol 279:736–739.

35. Cooper RR, Misol S. 1970. Tendon and ligament insertion. A light and electron microscopic study. J Bone Joint Surg Am 52:1–20.
36. Videman T. 1970. An experimental study of the effects of growth on the relationship of tendons and ligaments to bone at the site of diaphyseal insertion. Acta Orthop Scand Suppl 131:7–21.
37. Woo SL, Gomez MA, Seguchi Y, et al. 1983. Measurement of mechanical properties of ligament substance from a bone-ligament-bone preparation. J Orthop Res 1: 22–29.
38. Moffat KL, Chahine NO, Hung CT, et al. 2005. Characterization of the mechanical properties of the ACL–Bone insertion. American Society of Mechanical Engineers Summer Bioengineering Conference.
39. Hoyte DA, Enlow DH. 1966. Wolff's law and the problem of muscle attachment on resorptive surfaces of bone. Am J Phys Anthropol 24:205–213.
40. Spalazzi JP, Gallina J, Fung-Kee-Fung SD, et al. 2006. Elastographic imaging of strain distribution in the anterior cruciate ligament and at the ligament-bone insertions. J Orthop Res (in press).
41. Fujioka H, Wang OJ, et al. 1997. Changes in the expression of type-X colllagen in the fibrocartilage of rat Achilles tendon attachment during development. J Orthop Res 15:675–681.